

ORIGINAL ARTICLE

# Effects of p38 $\alpha$ / $\beta$ inhibition on acute lymphoblastic leukemia proliferation and survival *in vivo*

A Alsadeq<sup>1</sup>, S Strube<sup>1</sup>, S Krause<sup>1</sup>, M Carlet<sup>2</sup>, I Jeremias<sup>2</sup>, C Vokuhl<sup>3</sup>, S Loges<sup>4</sup>, JA Aguirre-Ghiso<sup>5,6</sup>, A Trauzold<sup>7</sup>, G Cario<sup>1</sup>, M Stanulla<sup>8</sup>, M Schrappe<sup>1</sup> and DM Schewe<sup>1</sup>

P38 $\alpha$ / $\beta$  has been described as a tumor-suppressor controlling cell cycle checkpoints and senescence in epithelial malignancies. However, p38 $\alpha$ / $\beta$  also regulates other cellular processes. Here, we describe a role of p38 $\alpha$ / $\beta$  as a regulator of acute lymphoblastic leukemia (ALL) proliferation and survival in experimental ALL models. We also report first evidence that p38 $\alpha$ / $\beta$  phosphorylation is associated with the occurrence of relapses in TEL-AML1-positive leukemia. First, *in vitro* experiments show that p38 $\alpha$ / $\beta$  signaling is induced in a cyclical manner upon initiation of proliferation and remains activated during log-phase of cell growth. Next, we provide evidence that growth-permissive signals in the bone marrow activate p38 $\alpha$ / $\beta$  in a novel avian ALL model, in which therapeutic targeting can be tested. We further demonstrate that p38 $\alpha$ / $\beta$  inhibition by small molecules can suppress leukemic expansion and prolong survival of mice bearing ALL cell lines and primary cells. Knockdown of p38 $\alpha$  strongly delays leukemogenesis in mice xenografted with cell lines. Finally, we show that in xenografted TEL-AML1 patients, *ex vivo* p38 $\alpha$ / $\beta$  phosphorylation is associated with an inferior long-term relapse-free survival. We propose p38 $\alpha$ / $\beta$  as a mediator of proliferation and survival in ALL and show first preclinical evidence for p38 $\alpha$ / $\beta$  inhibition as an adjunct approach to conventional therapies.

Leukemia (2015) 29, 2307–2316; doi:10.1038/leu.2015.153

## INTRODUCTION

The prognosis of childhood acute lymphoblastic leukemia (ALL) has improved over the last decades because of permanent refinement of treatment in clinical trials. Nevertheless, 15% of the patients suffer from relapse<sup>1</sup> making relapsed ALL a leading cause of cancer-related death in pediatrics.<sup>2</sup> Relapses in patients with favorable cytogenetics such as TEL-AML1 are particularly devastating to patients and physicians as they often occur long after termination of therapy and are unpredictable.<sup>3</sup> Unlike in other hematological malignancies, targeted approaches aiming to increase therapy specificity are limited. These findings emphasize the need for new diagnostic and therapeutic strategies further improving long-term outcomes.

Several preclinical studies have shown that p38 inhibition abrogates stroma-dependent pro-proliferative signals<sup>4,5</sup> in multiple myeloma, which is also a B-cell malignancy. ALL cells rely on niche-dependent growth signals as well, which may explain why culturing primary ALL samples *in vitro* is difficult.<sup>6</sup> It has, for instance, been demonstrated that the production of pro-proliferative cytokines in co-cultures of ALL cells with bone marrow mesenchymal stromal cells, such as C-X-C motif ligand 12, interleukin-6, vascular endothelial growth factor and platelet-derived growth factor, is p38 dependent.<sup>7</sup> However, these stromal cells are often immortalized, which questions whether observations from co-culture models indeed reflect the *in vivo* situation.

The p38 family of mitogen-activated protein kinases (MAPKs) consists of four isoforms ( $\alpha$ ,  $\beta$ ,  $\gamma$ ,  $\delta$ ) with partly redundant

functions. P38 MAPKs are induced by stress insults and inflammatory cytokines<sup>8</sup> and regulate downstream pathways involved in cell proliferation and survival. Two major groups of targets are activated by p38: transcription factors, such as p53 and ATF-2, and protein kinases, such as MAPK-activated protein kinase 2 (MAPKAPK2), which leads to the phosphorylation of heat-shock protein Hsp27 during stress responses.<sup>8</sup> In normal hematopoiesis, p38 has been associated with growth-inhibitory signals.<sup>9</sup> In addition, p38 $\alpha$  has been shown to regulate dormancy in experimental head and neck cancer models via an activation of transcription factors accounting for specific cellular functions.<sup>10,11</sup> In lymphoid cells and in ALL, p38 $\alpha$ / $\beta$  has been shown to upregulate pro-apoptotic Bim in response to glucocorticoid therapy.<sup>12,13</sup> Similarly, in myelodysplastic syndromes, apoptosis of hematopoietic progenitors was p38-dependent and p38 inhibition induced the differentiation of these cells.<sup>14</sup> Last, p38 has been implicated in acting downstream of CXCR4 thereby regulating the homing of ALL cells to the bone marrow.<sup>15,16</sup>

Here, we show that p38 $\alpha$ / $\beta$  is cyclically phosphorylated during initiation of ALL cell growth *in vitro* and that it remains activated during log-phase of cell growth. We also provide evidence that p38 $\alpha$ / $\beta$  phosphorylation is associated with proliferation and survival *in vivo*. Targeting p38 $\alpha$ / $\beta$  signaling by different approaches prolongs survival of mice xenografted with ALL cells. TEL-AML1-positive pediatric patients with activated p38 $\alpha$ / $\beta$  signaling in xenografts suffer from late relapses, suggesting a pro-survival role in residual cells. Our data provide a rationale for

<sup>1</sup>Department of General Pediatrics, ALL-BFM Study Group, University Hospital Schleswig-Holstein, Kiel, Germany; <sup>2</sup>Helmholtz Zentrum München, Department of Gene Vectors, Research Center for Environmental Health, Munich, Germany; <sup>3</sup>Kiel Pediatric Tumor Registry, Department of Pediatric Pathology, University of Kiel, Kiel, Germany; <sup>4</sup>II. Medical Clinic and Institute of Tumor Biology, University Hospital Eppendorf, Hamburg, Germany; <sup>5</sup>Division of Hematology and Oncology, Department of Medicine, Mount Sinai School of Medicine, New York, NY, USA; <sup>6</sup>Department of Otolaryngology, Mount Sinai School of Medicine, New York, NY, USA; <sup>7</sup>Division of Molecular Oncology, Institute for Experimental Cancer Research, University of Kiel, Kiel, Germany and <sup>8</sup>Department of Pediatric Hematology/Oncology, Hannover Medical School, Hannover, Germany. Correspondence: Dr D Schewe, Department of General Pediatrics, ALL-BFM Study Group, University Hospital Schleswig-Holstein, 24105 Kiel, Germany. E-mail: denis.schewe@uksh.de

p38 $\alpha/\beta$  inhibition as a targeted therapy for ALL, which could be further evaluated in patients with activated p38 $\alpha/\beta$  signaling.

## MATERIALS AND METHODS

Detailed information is given in Supplementary Methods.

### Ethics statement

Studies in avian embryonal xenografts and animal studies were approved by the institutional ethics committee and the local government.

### Cell lines, plasmids, drugs and inhibitors

REH, 697 (EU-3) and SUP-B15 cells were purchased from DSMZ (Braunschweig, Germany), and 293T cells from American Type Culture Collection (ATCC/LGC Standards Germany, Wesel, Germany). Cell culture was performed according to the DSMZ recommendations.<sup>17</sup> Cell viability assays were performed using Trypan blue exclusion.

### Patient cells

Patient cells were from the ALL-BFM repository. Patients suffered from TEL-AML1-positive ALL and were treated according to the ALL-BFM 2000

**Table 1.** Characteristics of TEL-AML1-positive patients xenografted into NSG mice for analysis of p38 $\alpha/\beta$  phosphorylation

	p-p38 <sup>neg</sup> (n = 4)	p-p38 <sup>pos</sup> (n = 8)	P
Sex <sup>a</sup>		1.000	
Male	3	5	
Female	1	3	
Median age (range) at diagnosis (years) <sup>b</sup>	5.6 (4.7–13.3)	4.8 (2.7–7.4)	0.308
Immunophenotype <sup>a</sup>			1.000
Common-ALL	4	7	
Pre-B-ALL	0	1	
WBC count <sup>a</sup>			1.000
< 50 000/ $\mu$ l	2	5	
$\geq$ 50 000/ $\mu$ l	2	3	
Prednisone response <sup>a,c</sup>			1.000
Good	4	8	
Poor	0	0	
Risk group <sup>a,d</sup>			0.067
MRD-SR	3	1	
MRD-IR/-HR	1	7	
Extramedullary manifestation (initial) <sup>e</sup>			1.000
Yes	0	0	
No	4	8	
Relapse <sup>f</sup>			0.002
Yes	0	8	
No	4	0	
Death <sup>g</sup>			0.491
Yes	0	3	
No	4	5	

Abbreviations: ALL, acute lymphoblastic leukemia; B-ALL, B-cell ALL; MRD-HR, minimal residual disease-high risk; MRD-IR, minimal residual disease-intermediate risk; MRD-SR, minimal residual disease-standard risk; WBC, white blood cells. <sup>a</sup>Fisher's exact test, two-sided *P*-value. <sup>b</sup>Unpaired *t*-test with Welsh's correction. <sup>c</sup>Good: less than 1000 leukemic blood blasts/ $\mu$ l on treatment day 8, poor: more than 1000/ $\mu$ l. <sup>d</sup>Risk stratification according to MRD risk groups: MRD-SR: time point (TP) 1+2 negative, MRD-IR: TP1 and/or TP2 < 10<sup>-3</sup>, MRD-HR: TP2 > 10<sup>-3</sup>. <sup>e</sup>CNS 2/3 status, testicular involvement. <sup>f</sup>Five relapses were isolated bone marrow relapses. One relapse was a combined bone marrow/CNS relapse. One relapse was an isolated testicular relapse, one was an isolated CNS relapse. Two patients had two relapses, both of which were bone marrow relapses. <sup>g</sup>All deaths were related to the relapse. One patient died from pontine infarction at relapse, one from post-SCT bronchiolitis obliterans organizing pneumonia and one patient from sepsis.

protocol. Detailed information is given in Table 1. Informed consent was obtained according to the institutional regulations.

### Xenografts

Fertilized turkey embryos were obtained from Moorgut Kartzfehn (Bösel, Germany) and incubated in a humidified turning incubator (Brinsea, Sandford, UK). Detailed information is given in Supplementary Methods and Supplementary Figure 4. NSG mice (NOD.Cg-Prkdc<sup>scid</sup> Il2rg<sup>tm1Wjl/SzJ</sup>) were purchased from Charles River (Sulzfeld, Germany) and bred at our institution's animal care facility.

## RESULTS

### p38 $\alpha/\beta$ Phosphorylation correlates with ALL proliferation

To clarify the role of p38 $\alpha/\beta$  signaling in ALL cells, we screened ALL cell lines for p38 $\alpha/\beta$  phosphorylation under optimum culture conditions. Low or absent basal phosphorylation of p38 $\alpha/\beta$  after seeding was enhanced upon *in vitro* growth in 697 cells (E2A-PBX1 fusion gene), which have a doubling time of 30 h in medium with full serum (Figure 1a, left panel). The p-p38 $\alpha/\beta$  level reached a maximum after 48 h, representing log-phase of cell growth (Supplementary Figure 1A), and then started to decline as the cells reached high density beyond 72 h (Figure 1a, left panel). REH cells (TEL-AML1 fusion gene) have a doubling time of 50–60 h (Supplementary Figure 1A) and also induced phosphorylation of p38 $\alpha/\beta$  upon growth at later time points, most likely due to a slower proliferation rate (Figure 1b, right panel). An additional cell line, SUP-B15 cells (BCR-ABL1 fusion), showed no induction of p38 $\alpha/\beta$  phosphorylation (Supplementary Figure 1B). To obtain a more accurate assessment on the activation of p38 signaling in early stages of growth initiation, we analyzed p38 $\alpha/\beta$  phosphorylation in full serum conditions after the cycle was synchronized by serum starvation. P38 $\alpha/\beta$  phosphorylation was activated at 9 h after the addition of serum, declined after one population doubling and increased again during the next cell cycle at 30 h in 697 cells (Figure 1b, left panel). Interestingly, we detected persistent p-p38 $\alpha/\beta$  from 48 to 72 h, which, in 697 cells, represents log-phase of cell growth. From time points 75 to 96 h, 697 cultures reach confluence, impeding growth. This is reflected by a reduction in p-p38 $\alpha/\beta$  (Supplementary Figure 1C, left panel). Similarly, in REH cells displaying intermediate p38 $\alpha/\beta$  phosphorylation after seeding, which may be due to the stress of nutritional starvation, the first clear induction of p38 $\alpha/\beta$  phosphorylation was seen at 33 h (Figure 1b, right panel). In contrast to 697 cells, a further round of p38 $\alpha/\beta$  activation could be detected from 60 to 75 h, which is likely due to the lower proliferation rate in this cell line (Supplementary Figure 1C, right panel). In both cell lines, p38 $\alpha/\beta$  activation was accompanied by an overall decrease in p21 protein levels, which marks a blockade in G1–S transition (Figure 1b) and an increase in cells in S-phase as evidenced by 5-bromo-2-deoxyuridine (BrdU) staining (Figure 1c). These data suggest that despite the differences in p-p38 $\alpha/\beta$ , overall changes in the culture reflect increasing proliferation rates until confluence is reached. To clarify the cell cycle distribution in the subpopulation with highest p-p38 $\alpha/\beta$ , 697 cells were cultured in the presence of BrdU and studied by intracellular staining using 7-amino-actinomycin D and p-p38 $\alpha/\beta$  as well as anti-BrdU antibodies. After 24 h in culture, data was obtained in the 10% of 697 cells with the strongest phosphorylation of p38 $\alpha/\beta$  by flow cytometry (Figure 1d). These cells were gated as p-p38 $\alpha/\beta$ <sup>high</sup> and the remaining cells as p-p38 $\alpha/\beta$ <sup>low</sup>. Whereas 41.1% of the p-p38 $\alpha/\beta$ <sup>low</sup> cells were in G0/G1 phase, only 7.9% of the p-p38 $\alpha/\beta$ <sup>high</sup> cells were in G0/G1 in favor of the S- and G2/M-phases (Figure 1d). Our data show that the 697 and REH ALL cell lines cyclically activate p38 $\alpha/\beta$  phosphorylation during early stages of cell cycle progression and that p-p38 $\alpha/\beta$  then remains high during log-phase of cell growth. Our flow cytometry data support that p-p38 $\alpha/\beta$ <sup>high</sup> cells are dividing, which suggests a role for p38 $\alpha/\beta$  in

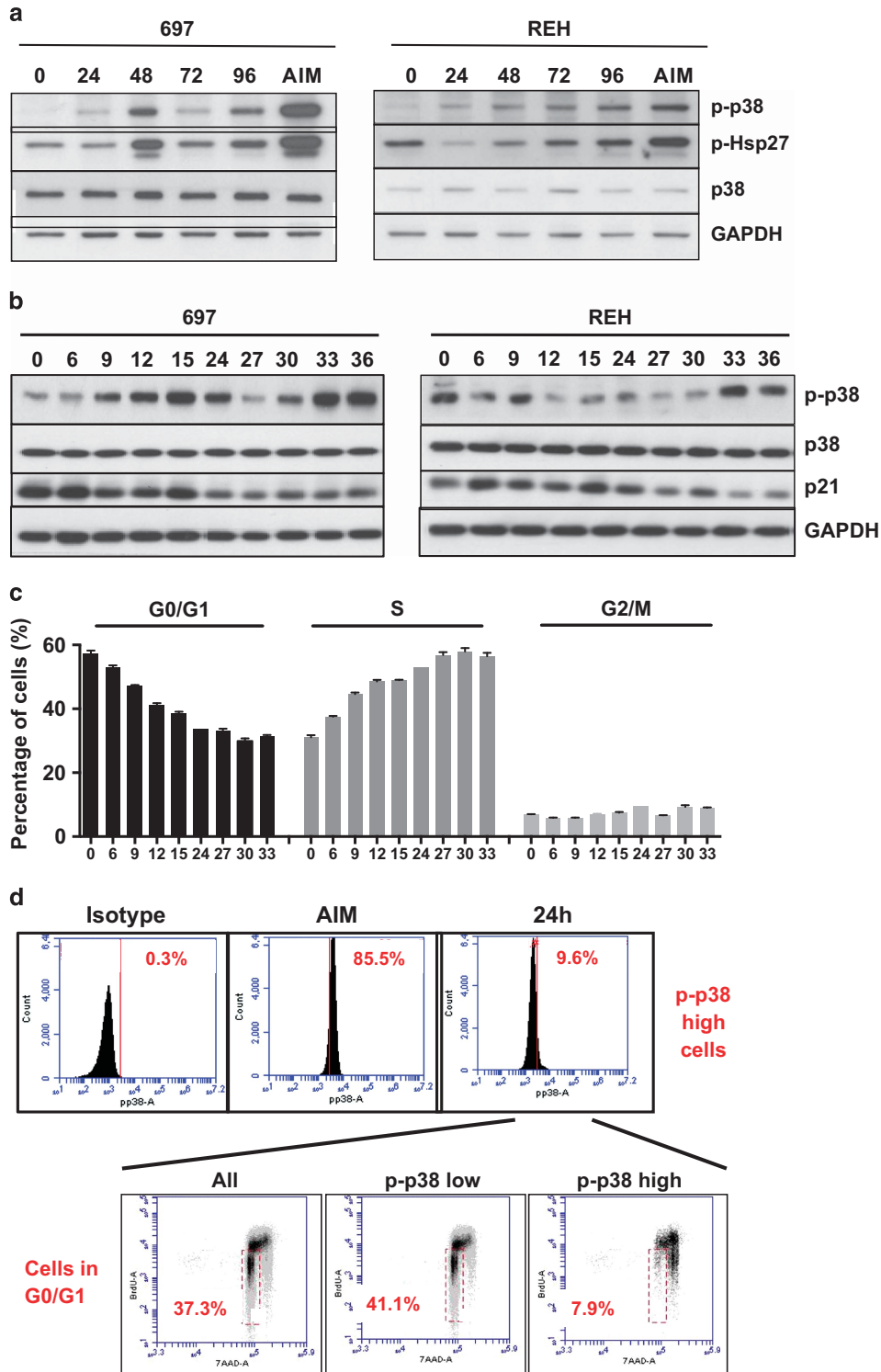


**Figure 1.** p38 $\alpha/\beta$  signaling upon ALL proliferation *in vitro*. **(a)** 697 cells (left panel) and REH cells (right panel) were cultured *in vitro* and assayed for p38 $\alpha/\beta$ - and Hsp27-phosphorylation by western blotting at different time points (0, 24, 48, 72 and 96 h, as indicated). Cells treated with 10  $\mu$ g/ml Anisomycin (AIM) for 15 min were processed in parallel as controls. **(b)** 697 cells (left panel) and REH cells (right panel) were serum starved for 24 h and then cultured in full serum conditions for the indicated time points. Western blotting was performed for p38 $\alpha/\beta$ , p38 $\alpha/\beta$ -phosphorylation, p21 and glyceraldehyde 3-phosphate dehydrogenase (GAPDH). **(c)** In parallel to the experiment in **b**, cells were allowed to incorporate BrdU for 1 h at the indicated time points and stained with 7-AAD and an anti-BrdU antibody. Cell cycle phases were determined by flow cytometry. **(d)** 697 cells were grown *in vitro* for 24 h, incubated with BrdU for 1 h and stained with a fluorescein isothiocyanate-labeled p-p38 $\alpha/\beta$  antibody or the respective isotype control. Subsequent staining with 7-AAD was also performed. After fluorescence-activated cell sorting analysis, the bulk of cells (All), p-p38 $\alpha/\beta$ -low and the 10% cells with highest p-p38 $\alpha/\beta$  (p-p38 $\alpha/\beta$ -high) were gated and cell cycle phases were assayed as indicated. Cells in G0/G1 are found in the red gate. 7-AAD, 7-amino-actinomycin D.

the S-phase. On the other hand, SUP-B15 cells proliferate in a p38 $\alpha/\beta$ -independent manner.

#### Inhibition of p38 $\alpha/\beta$ slows down ALL proliferation *in vitro*

The data above suggested that the activation of p38 $\alpha/\beta$  and its effector substrates have a pro-proliferative role in ALL cells. This raised the question whether p38 $\alpha/\beta$  inhibition would affect proliferation of ALL cells. Therefore, p38 $\alpha/\beta$  signaling was inhibited in 697 and REH cells using two p38-specific inhibitors: SB203580 and BIRB-796. SB203580 is an imidazole-type p38 $\alpha/\beta$ -specific inhibitor, which inhibits p38 catalytic activity by binding to the ATP-binding pocket. SB203580 has no activity against the p38 $\gamma/\delta$  isoforms.<sup>18</sup> Inhibition of catalytic activity does not prevent p38 $\alpha/\beta$  phosphorylation by upstream MAPK kinases (MAPKK), the phosphorylation may rather be increased due to feedback loops.<sup>19</sup> In contrast, BIRB-796 is a diaryl urea type inhibitor selective for all p38 isoforms<sup>20</sup> preventing both their catalytic activity and their activation by upstream MAPKKs.<sup>21</sup> The use of this compound showed efficiency in various cancer models<sup>4,22,23</sup> but it has entered only one randomized clinical trial for Crohn's disease.<sup>24</sup> We observed a dose-dependent deceleration of growth of up to

50% in 697 and REH cells with BIRB-796, which was marginally visible in SUP-B15 cells at 96 h only (Figure 2a and Supplementary Figure 2A, C and E). In REH cells, SB203580 effects were also dose dependent and, in 697 cells, all SB203580 doses equally reduced proliferation (Supplementary Figures 2B and D). SB203580 had no effects on SUP-B15 cells (Supplementary Figure 2F). To validate efficiency of the inhibitors, p-p38 and Hsp27 were analyzed after a 12-h (Supplementary Figure 1D) and a 48-h treatment (Figure 2b) in unsynchronized cultures. In REH cells, basal phosphorylation did not significantly change upon treatment, however, Anisomycin-inducible Hsp27 phosphorylation decreased in a dose-dependent manner (Figure 2b and Supplementary Figure 1D, left panels). In 697 cells, both basal and Anisomycin-inducible p-Hsp27 decreased at increasing inhibitor concentrations indicating a loss of p38 catalytic activity (Figure 2b and Supplementary Figure 1D, right panels). Our data also show that two inhibitors resulted in different phosphorylation patterns of p38 $\alpha/\beta$ . Cells treated with SB203580 exhibited an increase in p38 $\alpha/\beta$  at 48 h as this drug does not inhibit p38 $\alpha/\beta$  activation by upstream kinases persistently. In cells treated with BIRB-796, p38 $\alpha/\beta$  phosphorylation was decreased, as this drug is able to inhibit both p38 $\alpha/\beta$  activation

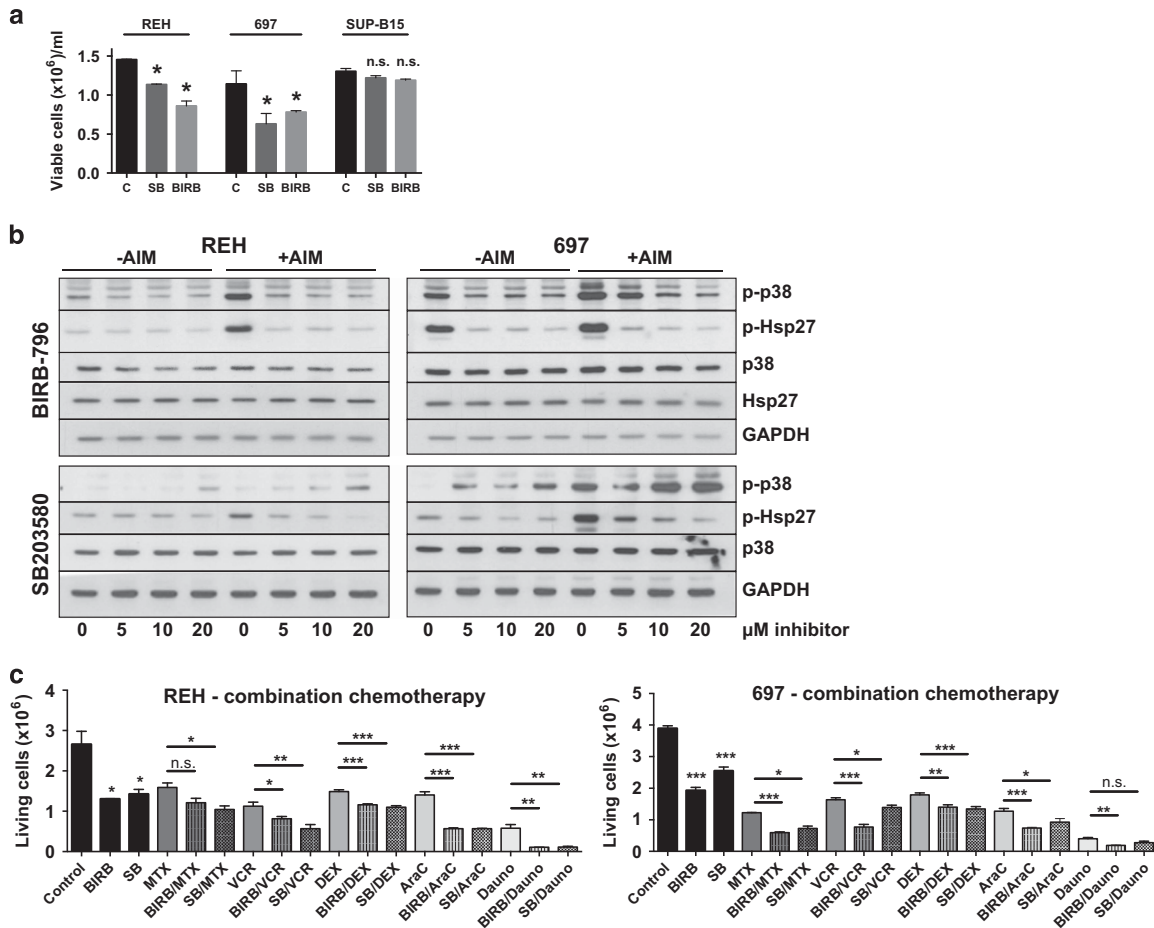


**Figure 2.** Cell counts and signaling upon p38 $\alpha/\beta$  inhibition *in vitro*. The experiments shown are representative experiments of at least two repetitions. (a) REH (left panel), 697 (middle panel) and SUP-B15 cells (right panel) were incubated with 10  $\mu$ M SB203580 (SB) or BIRB-796 (BIRB) for 72 h. The number of viable cells was counted using standard Trypan blue exclusion. \* $P < 0.05$ ; NS, not significant;  $t$ -test. (b) REH (left panel) and 697 cells (right panel) were incubated with ascending concentrations of BIRB-796 (upper panels) or SB203580 (lower panels) for 48 h. Dimethyl sulfoxide (0  $\mu$ M lanes) was used as a vehicle control. Cells were either directly lysed (- AIM) or stimulated with 10  $\mu$ g/ml Anisomycin for 15 min before lysis (+AIM). The indicated markers were assayed by western blotting. (c) REH (left panel) and 697 cells (right panel) were incubated with 20  $\mu$ M BIRB-796 (BIRB) or SB203580 (SB) alone or in combination with chemotherapeutic drugs for 48 h, as indicated. MTX, 30 nM Methotrexate (REH and 697); VCR, 1 nM (REH) and 2 nM (697) Vincristine; DEX, 100 nM (REH) and 50 nM (697) Dexamethasone; AraC, 50 nM Cytarabine (REH and 697); Dauno, 100 nM Daunorubicine (REH and 697). Standard chemotherapeutics were used at concentrations nearest to the IC<sub>50</sub> of the individual drug and cell line. Other concentrations are depicted in Supplementary Figure 3. \* $P < 0.05$ , \*\* $P < 0.01$ , \*\*\* $P < 0.001$ . C, control; GAPDH, glyceraldehyde 3-phosphate dehydrogenase.

and its activity. Interestingly, both inhibitors enhanced the effect of standard chemotherapeutics (Figure 2c and Supplementary Figure 3). For most combinations, at least one p38 inhibitor significantly intensified cytotoxicity of the standard drug (Figure 2c), which suggests that p38 $\alpha/\beta$  inhibition may be beneficial as an adjunct agent in all phases of therapy. Altogether, our data show that both SB203580 and BIRB-796 were efficient in inhibiting the p38 $\alpha/\beta$  pathway *in vitro*, particularly when stimulated with Anisomycin and that p38 $\alpha/\beta$  inhibitors may synergize with standard chemotherapy.

MAPK pathways are characterized by a high degree of crosstalk. If one pathway is inhibited, an alternative pathway is often activated.<sup>25</sup> For this reason, we analyzed if MAPK pathways, other than p38 $\alpha/\beta$ , were affected by p38 $\alpha/\beta$  inhibitors (Supplementary Figure 1E). REH cells showed no basal phosphorylation of extracellular signal-regulated kinase (ERK), but ERK was phosphorylated in 697 cells under basal conditions. After treatment with p38 $\alpha/\beta$  inhibitors, REH cells did not induce ERK-phosphorylation. However, 697 cells showed enhanced phosphorylation of ERK with both p38 $\alpha/\beta$  inhibitors, more notably with BIRB-796. Neither REH (Supplementary Figure 1E, left panel) nor 697 cells (right panel) showed any basal phosphorylation level of c-Jun N-terminal kinase (JNK) and p38 $\alpha/\beta$  inhibition did not induce JNK activation. These data show that the JNK pathway is functionally irrelevant to p38 inhibition in the ALL cell lines studied. On the other hand, there is crosstalk between p38 $\alpha/\beta$  and the ERK pathway in 697 cells but not in REH cells.

p38 $\alpha/\beta$  Phosphorylation is induced when ALL cells proliferate in the bone marrow of avian xenografts

Lymphoblasts are dependent on stroma-derived growth signals. Therefore, we hypothesized that the microenvironment in the bone marrow enhances ALL cell growth by inducing p38 signaling. To test this hypothesis, we established an avian xenograft model in embryonic turkeys. The avian model can be used for screening purposes before validation in mice because it is easy to handle, cost-efficient and offers a time window long enough for cellular engraftment. Previous studies have shown that a few hematological cell lines and samples from AML and multiple myeloma patients could engraft turkey embryos.<sup>26,27</sup> However, this model has not been used to study new therapeutic approaches or the function of signaling pathways. 697 cells constitutively expressing green fluorescent protein (GFP) were generated by retroviral transduction. To study p38 $\alpha/\beta$  activation *in vivo*, 697-GFP cells were injected into a large vessel of the turkey chorioallantoic membrane on day E11/12 (Supplementary Figure 4). On day E23, cells were recovered from the bone marrow and analyzed. First, lymphoblasts were isolated from BM and positively selected using human CD19 microbeads. The cells were then analyzed by western blotting (Figure 3a). P38 $\alpha/\beta$  phosphorylation was detected at low levels in cells cultured *in vitro* for 24 h, which also underwent magnetic-activated cell sorting separation (Figure 3a, left lane) and at high levels comparable to p-p38 $\alpha/\beta$  during log-phase of *in vitro* growth, in cells recovered from the avian bone marrow after 11–12 days (Figure 3a, right lane). Avian bone marrow cells from vehicle-injected embryos were processed in parallel and displayed similar p38 $\alpha/\beta$  phosphorylation and total p38 levels as 697 cells growing *in vitro* (Figure 3a, middle lane). This is likely due to the homology between the sequences of avian and human p38.<sup>28</sup> Furthermore, we performed an intracellular flow cytometry analysis of p-p38 $\alpha/\beta$  in 697-GFP cells immediately after their recovery from turkey bone marrows. Owing to the presence of nucleated avian erythrocytes in the *ex vivo* samples, all analyses were conducted using a primary lymphoblast and a secondary GFP gate. GFP-positive cells were analyzed and compared with respective *in vitro* controls with and without Anisomycin stimulation (Figure 3b). The 697-GFP cells cultured

*in vitro* exhibited 1% p-p38 $\alpha/\beta$  in this experiment, which was increased 16-fold after Anisomycin treatment. Interestingly, the cells that had passed through the avian bone marrow exhibited a 29-fold increase in p-p38 $\alpha/\beta$  levels (Figure 3b). Our data support the hypothesis that the avian bone marrow provides a pro-proliferative niche for 697 cells enhancing p38 $\alpha/\beta$  signaling.

Next, we tested the *in vivo* effects of p38 inhibition in the avian model. 697-GFP cells were injected into turkey embryos, which were treated with either SB203580 or dimethyl sulfoxide (DMSO; vehicle control) by intra-amniotic injection. We used SB203580, as it is soluble in DMSO, which is advantageous for proper absorption from the amniotic cavity. For non-xenograft viability controls, eight eggs were processed in parallel and were injected with saline and then treated with either SB203580 or DMSO. In the xenografted eggs, 3 out of 11 DMSO-treated embryos (27%) and 0 out of 9 SB203580-treated embryos died within the experiment. In the non-xenograft controls, 1 out of 4 DMSO-treated embryos (25%) and 0 out of 4 SB203580-treated embryos died (data not shown). On day E23, body weights of embryos were measured. Although the DMSO-treated xenografts had lower weights than all other groups, these differences were not statistically significant (Figure 3c, upper panel). However, engraftment of bone marrows by 697-GFP cells was threefold lower in SB203580-treated xenografts as shown by flow cytometry for GFP-positive cells (Figure 3c, lower panel). This result was confirmed by immunohistochemical staining of bones fixed in formalin. Conventional hematoxylin/eosin staining showed large patches of leukemic cells in the bone marrow of DMSO-treated xenografts, whereas only few cells or small patches were engrafted in SB203580-treated embryos (Figure 3d, upper panel). Staining for human CD19 confirmed that bone marrows of SB203580-treated embryos were interspersed with human leukemic cells as single cells or small islets. We finally verified target specificity by combinatorial immunohistochemical CD19 (purple)/p-Hsp27 (brown) staining. Whereas Hsp27-phosphorylation was strongly visible in DMSO-treated embryos (dark brown staining in Figure 3e, left panel), it was markedly reduced in SB203580-treated embryos as shown by the strong purple staining of CD19 (Figure 3e, right panel). Our results show that an intra-amniotic application of SB203580 suppresses p38 $\alpha/\beta$  signaling *in vivo*. Furthermore, the results suggest that p38 inhibition is an efficient treatment preventing ALL expansion in the bone marrow.

p38 $\alpha/\beta$  Inhibition by small molecules increases the survival of NSG xenografts and p38 $\alpha$  knockdown delays leukemogenesis

Our data have shown that p38 $\alpha/\beta$  is phosphorylated in ALL cells in the bone marrow, which is associated with proliferation. These findings were next validated in murine NSG xenografts. REH cells engineered to express a GFP construct were injected intravenously into mice. Animals were treated intraperitoneally with either SB203580 or with DMSO. Signs of systemic disease were delayed in the SB203580-treated animals, which resulted in a 25% prolongation of xenograft survival compared with the control group (median survival 54 versus 43 days,  $P=0.01$ , Figure 4a). This survival advantage in the treatment group was also present but less pronounced when treatment was initiated upon development of overt leukemia in the xenografts (Supplementary Figures 5A and B). To further corroborate our results using patient-derived material, xenograft spleen cells from a TEL-AML1-positive ALL patient (p-p38 $\alpha/\beta$  positive) were retransplanted into NSG mice. Mice treated intraperitoneally with SB203580 for >80 days showed significant neurotoxicity so that the experiment had to be terminated (data not shown). A similar experiment was thus performed using an orally available inhibitor. Mice were treated either with BIRB-796 or with the vehicle control by oral gavage. Clinical leukemia was delayed in the BIRB-796-treated animals resulting in a 49% increase in the survival time of this group

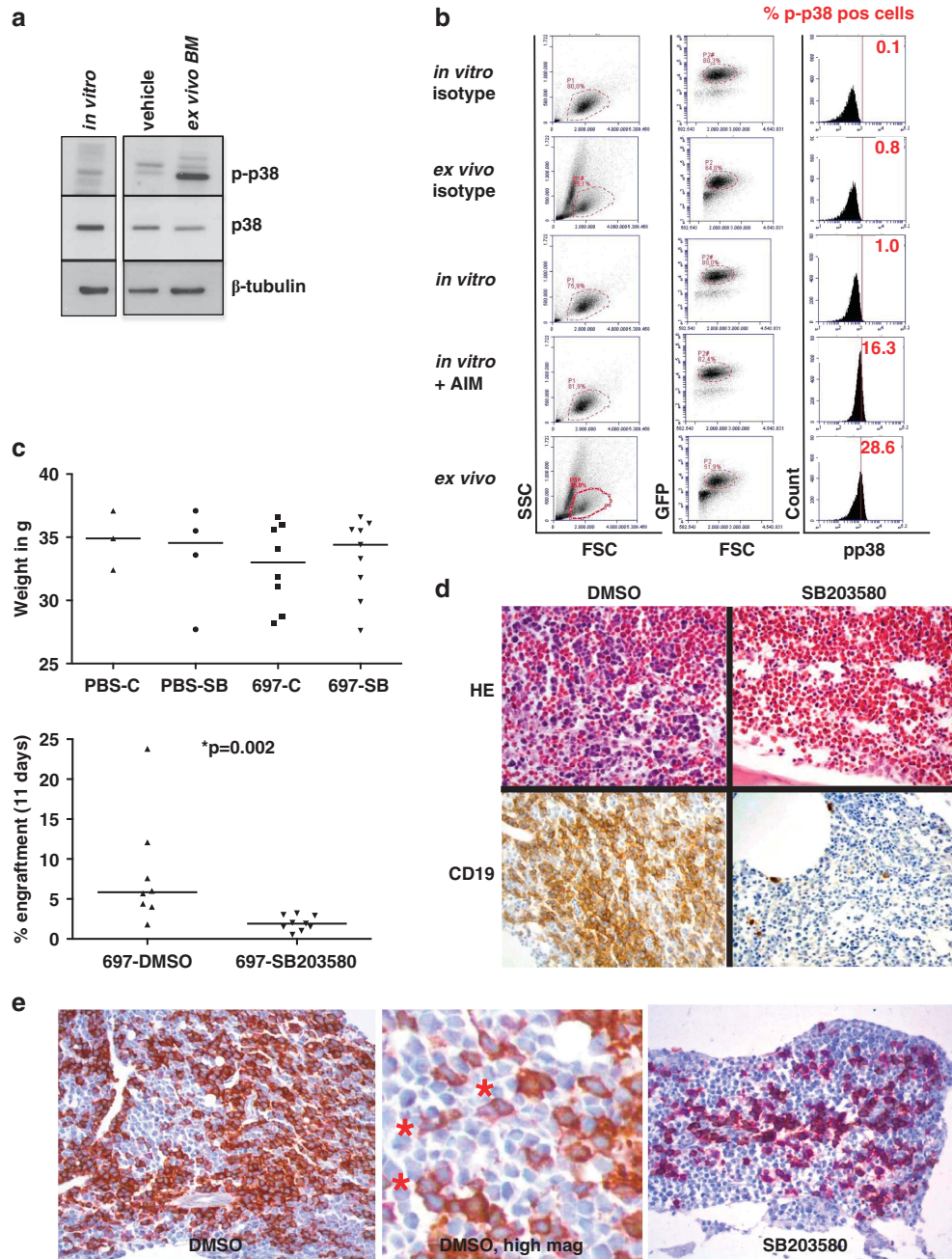


**Figure 3.** Induction of p38 $\alpha/\beta$  phosphorylation in 697 cells in the bone marrow of avian xenografts. **(a)** Cells cultured *in vitro* (lane 1) for 24 h after CD19 magnetic-activated cell sorting (MACS) and cells recovered from the bone marrow of a turkey embryo after 12 days *in vivo* (day E23) after CD19 MACS (lane 3) were subjected to western blot analysis for p38 $\alpha/\beta$  phosphorylation and total p38 levels. Bone marrow from a turkey embryo injected with phosphate-buffered saline (lane 2) was processed in parallel as a control. **(b)** 697-GFP cells were injected into turkey embryos and recovered from the bone marrow on day E23 (panels 2+5). 697-GFP cells were also cultured *in vitro* for 24 h in parallel (panels 1+3). Cells cultured *in vitro* for 24 h were induced with 10  $\mu\text{g}/\text{ml}$  Anisomycin (AIM) for 15 min (panel 4). Cells from all conditions were stained with a PE-labeled p-p38 $\alpha/\beta$  antibody. After fluorescence-activated cell sorting (FACS) analysis, cells were gated for the lymphoblast gate (P1) and then for GFP-positivity (P2 dependent on P1). Cells in the P2 gate were assayed for p38 $\alpha/\beta$  phosphorylation. The percentage of p-p38 $\alpha/\beta$ -positive cells is depicted in red. **(c)** 697-GFP cells were xenografted into turkey embryos as in **a**. Control eggs were injected with PBS. Eggs were treated with 10 mg/kg body weight SB203580 (SB) or 0.1% dimethyl sulfoxide as vehicle control every other day by intra-amniotic injection. Embryos were killed on day E23 by rapid decapitation, weighed and cells were recovered from the bone marrow of one femoral bone and assayed for GFP-positivity by FACS analysis. The upper panel shows the body weight in g in the respective groups. The lower panel shows engraftment as % GFP-positive cells with respect to all nucleated cells in the bone marrow. Nucleated cells in avian systems include erythrocytes. **(d)** The other femoral bone from **c** was fixed in formalin solution, embedded in paraffin, cut and stained by standard hematoxylin/eosin (HE) or immunohistochemistry for human CD19 (CD19). **(e)** Target specificity of p38 $\alpha/\beta$  inhibition assayed by double staining of p-Hsp27 (brown) and CD19 (purple). In DMSO-treated xenografts (left panel), a dark brown staining indicating p-Hsp27 positivity is evident, whereas in SB203580-treated xenografts (right panel), only purple staining is visible. The middle panel represents a digital high-magnification view showing CD19-positive purple cells also (\*).

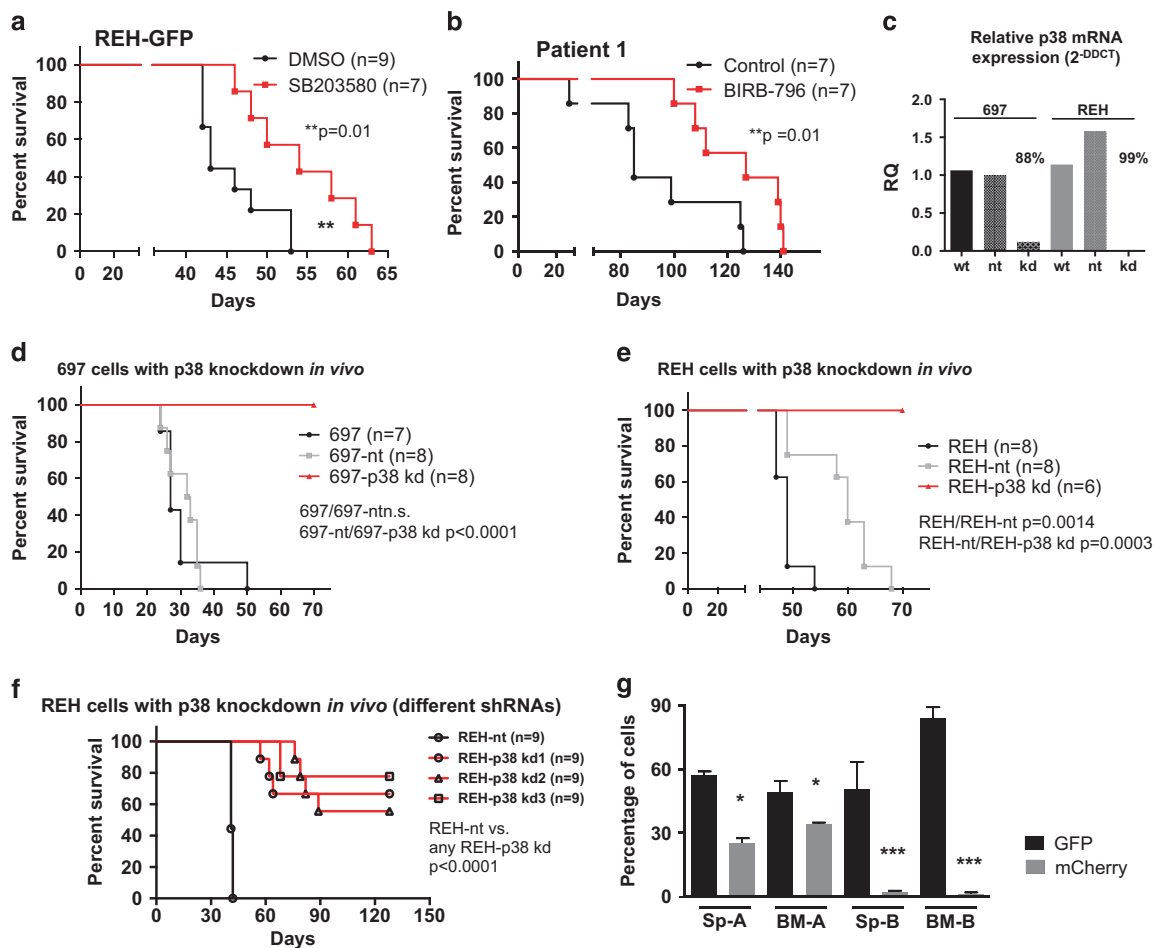


**Figure 4.** *In vivo* effects of p38 $\alpha/\beta$  inhibition. (a)  $1 \times 10^5$  REH-GFP cells/mouse were xenografted into NSG mice by tail vein injection. Animals were treated with 10 mg/kg SB203580 or DMSO 0.1% as vehicle control by intraperitoneal administration every other day. The graph depicts the respective survival curves. Statistics were performed according to the Mantel–Cox log-rank method. (b)  $1 \times 10^6$  cells from primary xenografts of a p-p38 $\alpha/\beta^{\text{high}}$  patient were xenografted into secondary mice by intrafemoral injection. Animals were treated with 10 mg/kg BIRB-796 or ethanol 2% in a 0.5% (w/w) hydroxypropylmethylcellulose solution as vehicle control by oral gavage 5 days/week. The graph depicts the respective survival curves. Statistics were performed according to the Mantel–Cox log-rank method. (c) Relative p38 mRNA expression levels of two replicate analyses as measured by the 2<sup>-DDCT</sup> method. Cells were measured before injection into mice. Non-targeting small hairpin RNA (shRNA) against GFP (nt), shRNA against p38 $\alpha$  (kd). Knockdown efficiency was calculated comparing nt and kd conditions. (d)  $1 \times 10^4$  697 cells with and without a p38 $\alpha$  knockdown were xenografted into NSG mice by intrafemoral injection as indicated. Animals were killed upon leukemic symptoms. The graph depicts the respective survival curves. Statistics were performed according to the Mantel–Cox log-rank method. (e)  $2 \times 10^4$  REH cells with and without a p38 $\alpha$  knockdown were xenografted into NSG mice by tail vein injection as indicated. Animals were killed upon leukemic symptoms. The graph depicts the respective survival curves. Statistics were performed according to the Mantel–Cox log-rank method. (f)  $5 \times 10^4$  REH cells with and without a p38 $\alpha$  knockdown (three further constructs, p38 kd(1), p38 kd(2) and p38 kd(3)) were xenografted into NSG mice by tail vein injection as indicated. Animals were killed upon leukemic symptoms. The graph depicts the respective survival curves. Statistics were performed according to the Mantel–Cox log-rank method. (g)  $1 \times 10^4$  697-GFP and  $1 \times 10^4$  697-nt (mCherry; group A) or  $1 \times 10^4$  697-GFP and  $1 \times 10^4$  697-p38 $\alpha/\beta$ -kd (mCherry; group B) cells were mixed and simultaneously xenografted into eight NSG mice per group by intrafemoral injection. Animals were killed upon leukemic symptoms. The graph depicts the fluorescence of spleen (Sp) and bone marrow (BM) leukemic blasts in groups A and B as indicated.

(median survival 127 vs 85 days,  $P=0.0126$ , Figure 4b). Importantly, both SB203580 and BIRB-796 efficiently reduced viability in cells of seven out of eight TEL-AML1-positive and also six out of six E2A-PBX1-positive patients recovered from xenografts *ex vivo* (Supplementary Figures 5C and D). Taken together, these data suggest that inhibition of p38 $\alpha/\beta$  is efficient in delaying leukemia onset and expansion in xenografts with REH cells and patient cells and in reducing *ex vivo* viability of primary ALL blasts.

To prove the specificity of the observed effects, we generated 697 and REH cell lines that constitutively express a small hairpin RNA against p38 $\alpha$ . Viral supernatants for the different constructs contained similar viral titers (Supplementary Figure 5E). The knockdown of p38 $\alpha$  was highly efficient in both cell lines as shown by quantitative PCR (Figure 4c). A slight induction of p38 $\alpha$  in

control REH cells may be due to a stress response to the infection procedure. Cells bearing p38 $\alpha$  knockdowns did not expand *in vitro* with one exception, in which the knockdown may have been partly lost (Supplementary Figures 5F and G). Next, lentivirally transduced cells were directly injected into NSG mice after fluorescence-activated cell sorting. Two control groups were used in this experiment: wild-type cells (wt) and cells transduced with a non-targeting control construct (nt). Animals with 697-wt and 697-nt cells died from systemic leukemia, or were killed due to clinical leukemia signs (median survival 27 and 32.5 days, respectively). All killed animals had leukemia as evidenced by microscopy and fluorescence-activated cell sorting analysis (data not shown). Importantly, the knockdown of p38 $\alpha$  (kd) resulted in a remarkable and sustained prolongation of xenograft survival beyond 70 days

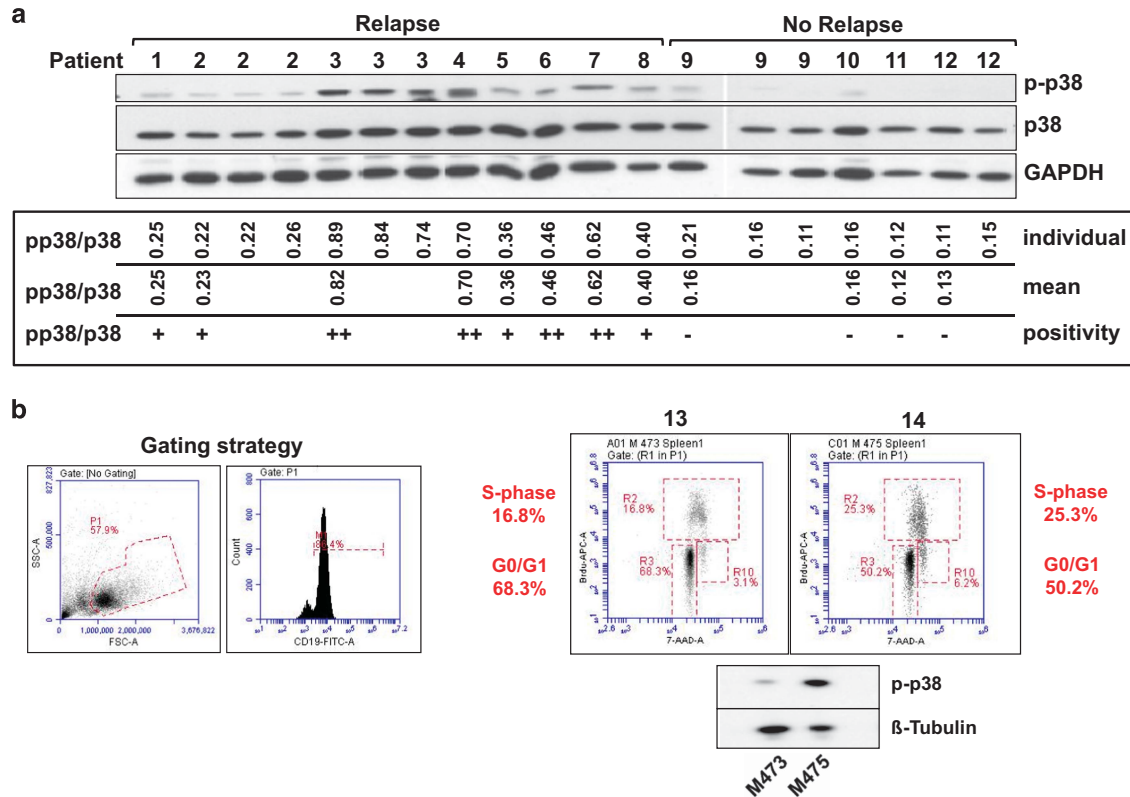


**Figure 5.** p38 $\alpha$ / $\beta$  phosphorylation is correlated with the occurrence of relapses in xenografted TEL-AML1-positive patient samples. **(a)** Initial bone marrow from 17 TEL-AML1-positive patients was xenografted into NSG mice. 12 patient samples engrafted a total of 20 mice and leukemic blasts from xenograft spleens were analyzed by western blotting for p38 $\alpha$ / $\beta$ , p38 $\alpha$ / $\beta$  phosphorylation and glyceraldehyde 3-phosphate dehydrogenase (GAPDH; upper panel). The p-p38 $\alpha$ / $\beta$ /p38 $\alpha$ / $\beta$  ratio was calculated using quantitation by Image J for each individual lane. Mean p-p38 $\alpha$ / $\beta$ /p38 $\alpha$ / $\beta$  ratios and p-p38 $\alpha$ / $\beta$ /p38 $\alpha$ / $\beta$  positivity are depicted for each individual patient. Patients with p-p38 $\alpha$ / $\beta$ /p38 $\alpha$ / $\beta$  ratios in the lowest tertile were considered negative, all others positive (+ or ++, as indicated). **(b)** Initial bone marrow cells from two further TEL-AML1-positive patients with relapses were xenografted into NSG mice. On day 90, mice were injected with BrdU intraperitoneally for 1 h and then killed. Spleen cells were harvested and subjected to protein lysis or combinatorial BrdU/7-AAD staining. The gating strategy is depicted in the left panel: lymphoblasts (P1) and CD19-positive cells (M1). The right panel depicts the cell cycle distribution in both samples and p-p38 $\alpha$ / $\beta$  levels as measured by western blotting. 7-AAD, 7-amino-actinomycin D.

in all animals (Figure 4d,  $P < 0.0001$ ). Although the mice injected with REH-nt cells survived longer than mice bearing REH-wt cells (median survival 60 and 49 days, respectively), they all showed symptoms of leukemia (Figure 4e,  $P = 0.0014$ ). Animals injected with REH-wt and REH-nt cells expectedly died from systemic leukemia later than 697 cells as these cells proliferate more slowly. Nevertheless, knockdown of p38 $\alpha$  in REH cells significantly prolonged animal survival as compared with the control cells (Figure 4e,  $P = 0.0003$ ). None of the animals transplanted with p38 $\alpha$  knockdown cells (Figures 4d and e) showed leukemic signs when they were killed and none of the mice showed evidence of leukemia by fluorescence-activated cell sorting or MRD-PCR (data not shown). The abrogation of leukemogenesis in xenografts was confirmed in an independent experiment with more REH-p38 $\alpha$  kd clones. Median survival was 41 days for REH-nt animals and  $> 50\%$  of the animals bearing any REH-p38 $\alpha$  kd clone were alive at 128 days (Figure 4f,  $P < 0.0001$ ). To confirm that p38 $\alpha$  knockdown indeed affects the survival of leukemic cells, we performed competitive transplantation experiments with 697 cells transduced with an MSCV-GFP construct or the p38 $\alpha$ -nt or p38 $\alpha$ -kd constructs (mCherry fluorescence). Equal numbers of 697-GFP and 697-p38 $\alpha$ -nt cells (group A) and equal numbers of 697-GFP and 697-p38 $\alpha$ -kd cells (group B) were transplanted into NSG mice simultaneously. All animals rapidly died from systemic leukemia at a median of 24 days in group A and 26 days in group B (data not shown). All animals in group A had leukemia with mixed fluorescence (GFP/mCherry), whereas all animals in group B had

a GFP-positive leukemia with  $< 5\%$  mCherry-positive cells in the spleen and the bone marrow (Figure 4g). These data suggest that p38 $\alpha$  is indispensable for the survival of 697 and REH cells in xenografts. Altogether, our data show that p38 $\alpha$ / $\beta$  signaling is required for the manifestation of systemic leukemia in murine xenografts, and that inhibiting this pathway may be a new therapeutic approach in childhood ALL.

First evidence that p38 $\alpha$ / $\beta$  phosphorylation is associated with an inferior relapse-free survival in xenografted TEL-AML1-positive pediatric ALL patients

To assess the levels of p38 $\alpha$ / $\beta$  phosphorylation in patient samples, initial bone marrows of 17 pediatric patients with TEL-AML1 fusion were injected intrafemorally into NSG mice. For our analyses, we chose a cohort of nine TEL-AML1-positive patients with late relapses at a median of 1346 days and of eight TEL-AML1-positive control patients in continuous complete remission for  $> 6$  years. Eight out of nine patients in the relapse and four out of eight patients in the control group engrafted in NSG mice within 40 weeks. Cells from engrafted spleens ( $> 90\%$  leukemic blasts) were freshly lysed and assessed for p-p38 $\alpha$ / $\beta$  by western blot (Figure 5). All eight patients in the relapse cohort showed p-p38 $\alpha$ / $\beta$ , whereas all four patients in the control cohort showed no phosphorylation of p38 $\alpha$ / $\beta$  as measured using Image J (Figure 5). The clinical data of all engrafted patients and correlation analyses with clinical parameters are shown in Table 1. Despite low sample numbers, we could detect a trend

between p38 $\alpha$ / $\beta$  phosphorylation and the MRD intermediate and high-risk groups as well as a statistically significant correlation between p-p38 $\alpha$ / $\beta$  and the occurrence of relapse (Table 1). Kaplan–Meier statistics confirmed a lower relapse-free survival in the patients showing p-p38 $\alpha$ / $\beta$  as compared with the controls ( $P=0.0037$ , data not shown). We next prepared independent xenografts from two further TEL-AML1-positive patients with relapses. On day 90, mice were subjected to *in vivo* BrdU incorporation. Splenic cells were harvested before full engraftment. Both *ex vivo* samples had p-p38 $\alpha$ / $\beta$ , but a higher intensity of p-p38 $\alpha$ / $\beta$  correlated with a larger percentage of leukemic cells in S-phase and a decrease in G0/G1 (Figure 5b). Taken together, these data provide first evidence that in TEL-AML1-positive ALL patient cells, p-p38 $\alpha$ / $\beta$  correlates with proliferative capacity and the occurrence of relapses.

## DISCUSSION

We found that p38 $\alpha$ / $\beta$  mediates pro-proliferative and pro-survival signals in ALL cells and that p38 $\alpha$ / $\beta$  signaling in these cells is activated *in vivo*. We showed that REH and 697 cells proliferate in a p38 $\alpha$ / $\beta$ -dependent manner, whereas SUP-B15 cells did not. This divergence may be due to the presence of the BCR-ABL1 fusion gene in SUP-B15 cells, which as a leukemic driver<sup>29</sup> may render cells more independent of niche-derived growth signals. In contrast, data on the role of the fusion genes in REH and 697 cells in cell cycle progression are inconclusive. An analysis of TEL-AML1 targets has shown that this fusion gene rather inhibits proliferation pathways,<sup>30</sup> which is supported by findings that TEL-AML1 is not implicated in ALL proliferation or survival.<sup>31</sup> On the other hand, studies have shown that TEL-AML1 induces a pre-leukemic clone with enhanced proliferation and survival properties in HSCs.<sup>32,33</sup> Furthermore, Fuka *et al.* advocate a role for this fusion in ALL proliferation and survival.<sup>34,35</sup> E2A-PBX1 causes a block in differentiation, but growth of E2A-PBX1-positive cells remains growth factor dependent.<sup>36</sup> It is thus likely that only some ALL entities are p38 $\alpha$ / $\beta$  dependent.

Even though a cyclical activation cannot be detected *in vivo*, we observed that the avian bone marrow causes high p38 signaling in 697 cells (Figures 3a and b), suggesting an influence of the niche. Treatment with a combination of interleukin-7 and C-X-C motif ligand 12 causes p38-mediated proliferation in primary ALL cells *in vitro*.<sup>15</sup> Furthermore, Gaundar *et al.*<sup>7</sup> have shown that in bone marrow mesenchymal stromal cells, the production of cytokines supporting ALL cell growth was p38 dependent. We thus advocate p38 $\alpha$ / $\beta$  inhibition as a double-hit strategy to inhibit stroma-derived cytokine production and an inherent proliferation mechanism in the ALL cell itself. P38 $\alpha$ / $\beta$  activation is frequently implicated in apoptotic signaling. It has been shown that p38 mediates glucocorticoid-induced apoptosis in some lymphoid cells.<sup>12,13,37,38</sup> This may be due to entity-specific differences as these data were generated in normal mouse lymphoid cells and in T-cell ALL (T-ALL). Conversely, it has also been implicated that p38 $\alpha$ / $\beta$  mediates interferon-induced growth-inhibitory signals in T-ALL.<sup>39</sup> Divergent p38 $\alpha$ / $\beta$  roles may be due to deviating receptor expression in a certain state of maturation arrest<sup>40</sup> or mutations upstream of p38 $\alpha$ / $\beta$ .<sup>41,42</sup> Our results support that for B-cell acute lymphoblastic leukemia cells bone marrow-derived signals determine the activation and subsequent function of p38 $\alpha$ / $\beta$ .

Experimental T-ALL created by expressing defective K-Ras proteins renders cells resistant to MEK inhibition *in vivo*.<sup>43</sup> To our knowledge, components of the p38 pathway are not mutated in leukemias, suggesting that p38 $\alpha$ / $\beta$  inhibition may be a potential therapy in all patients with a p38 $\alpha$ / $\beta$ <sup>high</sup> phenotype. In response to a MEK inhibitor, cells may turn on the PI3K/Akt pathway counteracting the desired apoptotic effect by a survival signal.<sup>43</sup> In our study, p38 $\alpha$ / $\beta$  inhibition lead to a slight activation of ERK in 697 cells, which lead to a reduction of viable cells (Figure 2a and Supplementary Figure 1E). In REH cells, p38 $\alpha$ / $\beta$  inhibition did not result in alterations

of ERK or JNK (Supplementary Figure 1E). Interestingly, in both cell lines, we could not detect any basal phosphorylation of JNK, and JNK was not induced when p38 $\alpha$ / $\beta$  was inhibited (Supplementary Figure 1E). JNK phosphorylation has been observed in T-ALL,<sup>44–47</sup> but its functional role remains unknown.

We used two approaches to inhibit p38 $\alpha$ / $\beta$ : small molecule and genetic inhibition. The main advantage of small-molecule inhibitors is their applicability *in vivo*.<sup>24</sup> However, small-molecule inhibitors are not as specific as genetic ablation of a target. We could show a prolongation in the survival times of xenografts when inhibitors were given (Figures 4a and b), but these drugs were not able to completely suppress leukemic growth. Also, SB203580 was more efficient when it was given early, supporting that p38 may have an important role in homing processes.<sup>15,16</sup> Limited efficiency of small-molecule inhibitors may additionally be due to the fact that optimum dosages, application schedules and routes for mice are unknown. The specific knockdown of p38 $\alpha$  by small hairpin RNA in our study was very efficient (Figure 4c) and abrogated or delayed the leukemogenic potential of REH and 697 in NSG xenografts (Figures 4d–f). This suggests that complete p38 $\alpha$ / $\beta$  inhibition may be desirable.

P38 $\alpha$ / $\beta$  inhibitors have been continuously developed but none has shown groundbreaking effects in malignancy. Surprisingly, in our small cohort of xenografted TEL-AML1-positive leukemia patients, we found *ex vivo* p38 $\alpha$ / $\beta$  phosphorylation to be restricted to relapsing patients (Figure 5). As TEL-AML1-positive leukemia encompasses up to 80% of all late relapses in pediatric ALL,<sup>48</sup> an identification of patients prone to this complication is of high clinical interest. We think that predictive measurements of p-p38 $\alpha$ / $\beta$  are difficult as phosphorylation events are susceptible to material degradation. Therefore, surrogates of p38 $\alpha$ / $\beta$  activation are needed in order to translate our findings into diagnostics. Our preclinical *in vivo* data suggest that a highly specific and potent p38 $\alpha$  inhibitor may be useful in inhibiting re-growth of residual cells but the fact that p38 can mediate glucocorticoid-induced apoptosis necessitates a cautious drug scheduling. P38 $\alpha$ / $\beta$  inhibitors could thus be included in maintenance therapy in p-p38 $\alpha$ / $\beta$ -positive ALL. Altogether, our data warrant further mechanistic studies and analyses on larger sets of primary patient samples in order to evaluate p38 $\alpha$ / $\beta$  inhibition as an adjunct approach to conventional therapy.

## CONFLICT OF INTEREST

The authors declare no conflict of interest.

## ACKNOWLEDGEMENTS

DMS and SL are supported by the Max-Eder group leader program by the Deutsche Krebshilfe e. V. DMS is supported by the Translational Research Training in Hematology Program 2014 by EHA and ASH. SL is further supported by the Deutsche Forschungsgemeinschaft (DFG), the Roggenbrück Stiftung, the Hamburger Krebsgesellschaft, the Medical Faculty of the University of Hamburg (FFM program) and the Hamburger Exzellenzinitiative (LEXI program). MC is supported by the Alexander von Humboldt Stiftung. IJ is supported by the Deutsche Forschungsgemeinschaft (SFB684, TP22) and the German José Carreras Leukemia Foundation (R10/26). JAA-G is supported by the Samuel Waxman Cancer Research Foundation Tumor Dormancy Program and NIH/National Cancer Institute grants (CA109182 and CA163131). We thank Katrin Timm-Richert, Katrin Neumann, Annika Brauer and Christian Bretscher for excellent technical assistance.

## AUTHOR CONTRIBUTIONS

DMS initiated, designed and supervised the research, analyzed the data and wrote the manuscript. SS and AA designed and performed experiments and analyzed the data. SK helped performing the experiments. CV performed the experiments and analyzed the data. MC and IJ contributed important constructs and professional expertise to the project. SL, GC, AT, JAA-G, M Stanulla and M Schrappe commented and discussed the research direction and edited the manuscript. All authors discussed the manuscript.

## REFERENCES

- Moricke A, Zimmermann M, Reiter A, Henze G, Schrauder A, Gadner H *et al.* Long-term results of five consecutive trials in childhood acute lymphoblastic leukemia performed by the ALL-BFM study group from 1981 to 2000. *Leukemia* 2010; **24**: 265–284.
- Locatelli F, Schrappe M, Bernardo ME, Rutella S. How I treat relapsed childhood acute lymphoblastic leukemia. *Blood* 2012; **120**: 2807–2816.
- Gandemer V, Chevret S, Petit A, Vermilyen C, Leblanc T, Michel G *et al.* Excellent prognosis of late relapses of ETV6/RUNX1-positive childhood acute lymphoblastic leukemia: lessons from the FRALLE 93 protocol. *Haematologica* 2012; **97**: 1743–1750.
- Yasui H, Hideshima T, Ikeda H, Jin J, Ocio EM, Kiziltepe T *et al.* BIRB 796 enhances cytotoxicity triggered by bortezomib, heat shock protein (Hsp) 90 inhibitor, and dexamethasone via inhibition of p38 mitogen-activated protein kinase/Hsp27 pathway in multiple myeloma cell lines and inhibits paracrine tumour growth. *Br J Haematol* 2007; **136**: 414–423.
- Wen J, Feng Y, Huang W, Chen H, Liao B, Rice L *et al.* Enhanced antitymoma cytotoxicity by the combination of arsenic trioxide and bortezomib is further potentiated by p38 MAPK inhibition. *Leukemia Res* 2010; **34**: 85–92.
- Nijmeijer BA, Suzhai K, Goselink HM, van Schie ML, van der Burg M, de Jong D *et al.* Long-term culture of primary human lymphoblastic leukemia cells in the absence of serum or hematopoietic growth factors. *Exp Hematol* 2009; **37**: 376–385.
- Gaundar SS, Bradstock KF, Bendall LJ. p38MAPK inhibitors attenuate cytokine production by bone marrow stromal cells and reduce stroma-mediated proliferation of acute lymphoblastic leukemia cells. *Cell Cycle* 2009; **8**: 2975–2983.
- Cuadrado A, Nebreda AR. Mechanisms and functions of p38 MAPK signalling. *Biochem J* 2010; **429**: 403–417.
- Verma A, Deb DK, Sassano A, Uddin S, Varga J, Wickrema A *et al.* Activation of the p38 mitogen-activated protein kinase mediates the suppressive effects of type I interferons and transforming growth factor-beta on normal hematopoiesis. *J Biol Chem* 2002; **277**: 7726–7735.
- Sosa MS, Avivar-Valderas A, Bragado P, Wen HC, Aguirre-Ghiso JA. ERK1/2 and p38alpha/beta signaling in tumor cell quiescence: opportunities to control dormant residual disease. *Clin Cancer Res* 2011; **17**: 5850–5857.
- Adam AP, George A, Schewe D, Bragado P, Iglesias BV, Ranganathan AC *et al.* Computational identification of a p38SAPK-regulated transcription factor network required for tumor cell quiescence. *Cancer Res* 2009; **69**: 5664–5672.
- Lu J, Quearry B, Harada H. p38-MAP kinase activation followed by BIM induction is essential for glucocorticoid-induced apoptosis in lymphoblastic leukemia cells. *FEBS Lett* 2006; **580**: 3539–3544.
- Zhao YN, Guo X, Ma ZG, Gu L, Ge J, Li Q. Pro-apoptotic protein BIM in apoptosis of glucocorticoid-sensitive and -resistant acute lymphoblastic leukemia CEM cells. *Med Oncol* 2011; **28**: 1609–1617.
- Zhou L, Opalinska J, Verma A. p38 MAP kinase regulates stem cell apoptosis in human hematopoietic failure. *Cell Cycle* 2007; **6**: 534–537.
- Juarez J, Baraz R, Gaundar S, Bradstock K, Bendall L. Interaction of interleukin-7 and interleukin-3 with the CXCL12-induced proliferation of B-cell progenitor acute lymphoblastic leukemia. *Haematologica* 2007; **92**: 450–459.
- Juarez JG, Thien M, Dela Pena A, Baraz R, Bradstock KF, Bendall LJ. CXCR4 mediates the homing of B cell progenitor acute lymphoblastic leukaemia cells to the bone marrow via activation of p38MAPK. *Br J Haematol* 2009; **145**: 491–499.
- Drexler HG. *Guide to Leukemia-Lymphoma Cell Lines*. Electronic Book, DSMZ: Braunschweig, Germany, 2010, p2.
- Nebreda AR, Porras A. p38 MAP kinases: beyond the stress response. *Trends Biochem Sci* 2000; **25**: 257–260.
- Kumar S, Jiang MS, Adams JL, Lee JC. Pyridinylimidazole compound SB 203580 inhibits the activity but not the activation of p38 mitogen-activated protein kinase. *Biochem Biophys Res Commun* 1999; **263**: 825–831.
- Kuma Y, Sabio G, Bain J, Shiro N, Marquez R, Cuenda A. BIRB796 inhibits all p38 MAPK isoforms *in vitro* and *in vivo*. *J Biol Chem* 2005; **280**: 19472–19479.
- Sullivan JE, Holdgate GA, Campbell D, Timms D, Gerhardt S, Breed J *et al.* Prevention of MKK6-dependent activation by binding to p38alpha MAP kinase. *Biochemistry* 2005; **44**: 16475–16490.
- He D, Zhao XQ, Chen XG, Fang Y, Singh S, Talele TT *et al.* BIRB796, the inhibitor of p38 mitogen-activated protein kinase, enhances the efficacy of chemotherapeutic agents in ABCB1 overexpression cells. *PLoS One* 2013; **8**: e54181.
- Carter TA, Wodicka LM, Shah NP, Velasco AM, Fabian MA, Treiber DK *et al.* Inhibition of drug-resistant mutants of ABL, KIT, and EGF receptor kinases. *Proc Natl Acad Sci USA* 2005; **102**: 11011–11016.
- Schreiber S, Feagan B, D'Haens G, Colombel JF, Geboes K, Yurcov M *et al.* Oral p38 mitogen-activated protein kinase inhibition with BIRB 796 for active Crohn's disease: a randomized, double-blind, placebo-controlled trial. *Clin Gastroenterol Hepatol* 2006; **4**: 325–334.
- Aguirre-Ghiso JA, Estrada Y, Liu D, Ossowski L. ERK (MAPK) activity as a determinant of tumor growth and dormancy; regulation by p38(SAPK). *Cancer Res* 2003; **63**: 1684–1695.
- Farnoushi Y, Cipok M, Kay S, Jan H, Ohana A, Naparstek E *et al.* Rapid *in vivo* testing of drug response in multiple myeloma made possible by xenograft to turkey embryos. *Br J Cancer* 2011; **105**: 1708–1718.
- Grinberg I, Reis A, Ohana A, Taizi M, Cipok M, Tavor S *et al.* Engraftment of human blood malignancies to the turkey embryo: a robust new *in vivo* model. *Leuk Res* 2009; **33**: 1417–1426.
- Dalloul RA, Long JA, Zimin AV, Aslam L, Beal K, Blomberg Le A *et al.* Multi-platform next-generation sequencing of the domestic turkey (*Meleagris gallopavo*): genome assembly and analysis. *PLoS Biol* 2010; **8**: e1000475.
- Mullighan CG. The molecular genetic makeup of acute lymphoblastic leukemia. *Hematol Am Soc Hematol Educ Program* 2012; **2012**: 389–396.
- Linka Y, Ginzl S, Kruger M, Novosel A, Gombert M, Kremmer E *et al.* The impact of TEL-AML1 (ETV6-RUNX1) expression in precursor B cells and implications for leukaemia using three different genome-wide screening methods. *Blood Cancer J* 2013; **3**: e151.
- Zaliova M, Madzo J, Cario G, Trka J. Revealing the role of TEL/AML1 for leukemic cell survival by RNAi-mediated silencing. *Leukemia* 2011; **25**: 313–320.
- Hong D, Gupta R, Ancliff P, Atzberger A, Brown J, Soneji S *et al.* Initiating and cancer-propagating cells in TEL-AML1-associated childhood leukemia. *Science* 2008; **319**: 336–339.
- Schindler JW, Van Buren D, Foudi A, Krejci O, Qin J, Orkin SH *et al.* TEL-AML1 corrupts hematopoietic stem cells to persist in the bone marrow and initiate leukemia. *Cell Stem Cell* 2009; **5**: 43–53.
- Fuka G, Kauer M, Kofler R, Haas OA, Panzer-Grumayer R. The leukemia-specific fusion gene ETV6/RUNX1 perturbs distinct key biological functions primarily by gene repression. *PLoS One* 2011; **6**: e26348.
- Fuka G, Kantner HP, Grausenburger R, Inthal A, Bauer E, Krapp G *et al.* Silencing of ETV6/RUNX1 abrogates PI3K/AKT/mTOR signaling and impairs reconstitution of leukemia in xenografts. *Leukemia* 2012; **26**: 927–933.
- Kamps MP, Wright DD. Oncoprotein E2A-Pbx1 immortalizes a myeloid progenitor in primary marrow cultures without abrogating its factor-dependence. *Oncogene* 1994; **9**: 3159–3166.
- Miller AL, Webb MS, Copik AJ, Wang Y, Johnson BH, Kumar R *et al.* p38 Mitogen-activated protein kinase (MAPK) is a key mediator in glucocorticoid-induced apoptosis of lymphoid cells: correlation between p38 MAPK activation and site-specific phosphorylation of the human glucocorticoid receptor at serine 211. *Mol Endocrinol* 2005; **19**: 1569–1583.
- Heidari N, Miller AV, Hicks MA, Marking CB, Harada H. Glucocorticoid-mediated BIM induction and apoptosis are regulated by Runx2 and c-Jun in leukemia cells. *Cell Death Dis* 2012; **3**: e349.
- Lee WH, Liu FH, Lee YL, Huang HM. Interferon-alpha induces the growth inhibition of human T-cell leukaemia line Jurkat through p38alpha and p38beta. *J Biochem* 2010; **147**: 645–650.
- Taguchi T, Kiyokawa N, Mimori K, Suzuki T, Sekino T, Nakajima H *et al.* Pre-B cell antigen receptor-mediated signal inhibits CD24-induced apoptosis in human pre-B cells. *J Immunol* 2003; **170**: 252–260.
- Shochat C, Tal N, Bandapalli OR, Palmi C, Ganmore I, te Kronnie G *et al.* Gain-of-function mutations in interleukin-7 receptor-alpha (IL7R) in childhood acute lymphoblastic leukemias. *J Exp Med* 2011; **208**: 901–908.
- Zenatti PP, Ribeiro D, Li W, Zuurbier L, Silva MC, Paganin M *et al.* Oncogenic IL7R gain-of-function mutations in childhood T-cell acute lymphoblastic leukemia. *Nat Genet* 2011; **43**: 932–939.
- Shieh A, Ward AF, Donlan KL, Harding-Theobald ER, Xu J, Mullighan CG *et al.* Defective K-Ras oncoproteins overcome impaired effector activation to initiate leukemia *in vivo*. *Blood* 2013; **121**: 4884–4893.
- Cui J, Wang Q, Wang J, Lv M, Zhu N, Li Y *et al.* Basal c-Jun NH2-terminal protein kinase activity is essential for survival and proliferation of T-cell acute lymphoblastic leukemia cells. *Mol Cancer Ther* 2009; **8**: 3214–3222.
- Chiarini F, Del Sole M, Mongiorgi S, Gaboardi GC, Cappellini A, Mantovani I *et al.* The novel Akt inhibitor, perifosine, induces caspase-dependent apoptosis and downregulates P-glycoprotein expression in multidrug-resistant human T-acute leukemia cells by a JNK-dependent mechanism. *Leukemia* 2008; **22**: 1106–1116.
- Scupoli MT, Donadelli M, Cioffi F, Rossi M, Perbellini O, Malpeli G *et al.* Bone marrow stromal cells and the upregulation of interleukin-8 production in human T-cell acute lymphoblastic leukemia through the CXCL12/CXCR4 axis and the NF-kappaB and JNK/AP-1 pathways. *Haematologica* 2008; **93**: 524–532.
- Leung KT, Li KK, Sun SS, Chan PK, Ooi VE, Chiu LC. Activation of the JNK pathway promotes phosphorylation and degradation of BimEL—a novel mechanism of chemoresistance in T-cell acute lymphoblastic leukemia. *Carcinogenesis* 2008; **29**: 544–551.
- Forestier E, Heyman M, Andersen MK, Autio K, Blennow E, Borgstrom G *et al.* Outcome of ETV6/RUNX1-positive childhood acute lymphoblastic leukaemia in the NOPHO-ALL-1992 protocol: frequent late relapses but good overall survival. *Br J Haematol* 2008; **140**: 665–672.

Supplementary Information accompanies this paper on the Leukemia website (<http://www.nature.com/leu>)